Proceedings of the Korean Nuclear Society Autumn Meeting
Taejon, Korea, October 2000

Evaluation of Very High CHF for Subcooled Flow Boiling Using an Artificial Neural Network and Mechanistic Models

Young Min Kwon*
Korea Atomic Energy Research Institute (KAERI)
150 Dukjin, Yusong, Taejon, Korea

Soon Heung Chang
Korea Advanced Institute of Science and Technology (KAIST)
371-3 Kusong, Yusong, Taejon, Korea

Abstract

A critical heat flux (CHF) prediction method using an artificial neural network (ANN) was evaluated for application to the high-heat-flux (HHF) subcooled flow boiling. The developed ANN predictions were compared with the experimental database consisting of a total of 3069 CHF data points. Also, the prediction performance by the ANN was compared with those by mechanistic models and a look up table technique. The parameter ranges of the experimental data are: $0.33 \leq D \leq 37.5$ mm, $0.002 \leq L \leq 4$ m, $0.37 \leq G \leq 134$ Mg/m^{2}s, $0.1 \leq P \leq 20$ MPa, $50 \leq \Delta h_{sub,in} \leq 1660$ kJ/kg, and $1.1 \leq q_{CHF} \leq 276$ MW/m^2. It was found that 91.5% of the total data points were predicted within a ± 20% error band, which showed the best prediction performance among the existing CHF prediction methods considered. The ANN method is likely to be suitable for the HHF subcooled flow boiling CHF.

1. Introduction

A subcooled flow boiling with phase change has been shown capable of accommodating high heat transfer rates due to its enhanced heat transfer mechanism. The critical heat flux (CHF) in the subcooled water at a high mass flow rate and high subcooling is being studied by many researchers, since it is an important parameter for the design of high-heat-flux (HHF) removal systems. The heat transfer system should be operated to maintain the wall temperature safely below the CHF to avoid the possibility of tube burnout.

The CHF mechanism in the subcooled flow boiling is not well understood, though large numbers of theoretical and experimental studies have been carried out. Among the many existing mechanistic models available today, only a few models are applicable to the HHF subcooled flow boiling CHF. The authors' previous study [1] showed that the models of Celata et al. [2], Weisman and Pei [3], and Kwon and Chang [4] predicted the HHF subcooled flow boiling CHF while keeping reliable accuracy.

As one of the CHF prediction methods, an artificial neural network (ANN) has been recognized to provide a valuable methodology for processing experimental CHF data. The ANN can model complex systems without requiring the explicit formulation of the possible relationship that may exist between the variables. Recently, Yapo et al. [5] and Moon and Chang [6] applied the ANN to the CHF.

In this paper, the CHF prediction procedure using the ANN was developed for the HHF subcooled flow boiling, and its prediction performance was compared with those by the mechanistic models and the look-up table method.

2. CHF for the HHF Applications

Among the possible techniques for HHF removal, subcooled water flow boiling is considered to be a more attractive means for engineering purposes. The heat loads required in the electronic components cooling and light water reactor (LWR) are on the order of 1 MW/m^2, which can be removed without exceeding the CHF by using a relatively low mass velocity and low subcooled flow boiling. Some HHF systems, such as fusion reactor components, particle accelerator targets, high-power lasers, and rocket nozzles require a very high heat flux, i.e., one order of magnitude higher than LWRs. Particularly, fusion reactor components require a very high heat removal rate up to 80 MW/m^2. These systems are controlled under a constant heat flux condition, and the large increase in wall temperature may result in burnout of the cooling channel.

Motivated by the need in development as well as the safety analysis of HHF applications, extensive studies of high CHFs have been made during the past several decades. Bergles [7] performed some experiments to investigate the CHF and flow characteristics of highly subcooled flow boiling with a high mass velocity in small diameter tubes. He showed that the reduction of tube diameter led to a substantial increase in CHF. Nariai and Inasaka [8] systematically investigated the effect of tube diameter and tube length on the CHF. They observed an abnormality of the subcooled flow boiling in small diameter tubes with a high mass velocity. The actual void fraction measured was considerably lower than those estimated by the existing correlations or models. The reduced void fraction at the tube exit resulted in an increase of the CHF. Most recently, Mudawar and Bowers [9] obtained the highest CHF of 276 MW/m^2 among those reported in the literature for uniformly heated tubes.

A total of 3069 experimental CHF data for water subcooled flow boiling in uniformly heated tubes was selected. The selection criteria were that the equilibrium quality at the tube exit is less than zero and the CHF value is greater than 1 MW/m^2. The ranges of parameters for the data set selected from different references [9, 10-18] are presented in Table 1. The ENEA CHF database in the range of fusion reactor thermal hydraulics was collected by Celata et al. [18].

According to the results of the authors' study [19], the CHF database was simply classified into two categories based on tube inside diameter and mass velocity: the HMSD (High Mass velocity and Small Diameter) region for G ≥10 Mg/m^{2}s and D < 3 mm, and the normal region for G < 10 Mg/m^{2}s or D ≥ 3 mm. However, the actual value for the boundary could not be clarified in the initial assessment. The first category includes 843 out of 3069 data points and the second category includes the remaining 2226 data points.

3. CHF Prediction Methods

Up to the present, the prediction methods of the CHF have been developed in four

Table 1. Experimental CHF data for the HHF subcooled flow boiling

Parameter	No.	D (mm)	*L* (m)	*P* (MPa)	*G* (Mg/m^{2}s)	$\Delta h_{sub,in}$(kJ/kg)	q_{CHF}(MW/m^2)
Thompson et al.[10]	541	1.14 ~ 37.5	0.04 ~ 1.97	2.1 ~ 19.0	0.7 ~ 7.5	49 ~ 1659	1.1 ~ 14.8
Becker et al. [11]	101	6.0 ~ 10.0	0.4 ~ 3.0	3.04 ~ 20.0	0.37 ~ 6.98	648 ~ 1384	1.05 ~ 7.48
Zenkevich [12]	244	5.8 ~ 11.0	1.0 ~ 4.0	7.85 ~ 19.6	0.96 ~ 5.06	239 ~ 1617	1.05 ~ 7.29
Chen et al. [13]	109	10.0 ~ 16.0	0.3 ~ 0.4	0.15 ~ 1.7	1.4 ~ 13.4	228 ~ 701	4.17 ~ 14.56
Boyd [14 - 16]	23	10.2	0.5 ~ 1.17	0.45 ~ 1.6	1.14 ~ 7.45	544 ~ 772	1.53 ~ 11.5
Nariai et al. [17]	14	6.0	0.1	0.1 ~ 1.5	4.59 ~ 8.69	245 ~ 671	8.5 ~ 22.1
Mudawar et al. [9]	169	0.4 ~ 0.9	0.0045 ~ 0.03	0.25 ~ 17.2	5.0 ~ 134.0	322 ~ 1584	9.4 ~ 276
ENEA [18]	1868	0.33 ~ 25.4	0.002 ~ 0.61	0.09 ~ 8.41	0.93 ~ 90.0	88 ~ 1018	3.33 ~ 228
Total	3069	0.33 ~ 37.5	0.002 ~ 4.0	0.1 ~ 20.0	0.37 ~ 134	49 ~ 1659	1.05 ~ 276

parts: empirical correlations, graphical or look-up table techniques, an analytical model based on the CHF mechanism, and ANN techniques. The advantage of analytical models based on the CHF mechanism is that it would be easily improved and extended to a wide range of operating conditions. In this section, the mechanistic model and the ANN method are briefly described for HHF applications.

3.1 Mechanistic CHF Models

Owing to the limited understanding of two-phase flow structure near the CHF and complicated phenomena relating the CHF, mechanistic CHF models have been considered of secondary importance. The mechanistic CHF models are valuable to understand the physical nature of the CHF phenomenon rather than prediction accuracy. Most of the mechanistic CHF models are based on hypothetical assumptions regarding the flow structure of the near-wall when the heat flux approaches the CHF condition.

The models of Celata et al., Weisman and Pei, and Kwon and Chang were chosen to evaluate the prediction performance for the HHF CHF database. Figure 1 illustrates the concept of each mechanistic model in which the Celata-Katto et al. model is in principle similar to the Celata et al. model. The Weisman-Pei model [3] based on the bubble crowding mechanism, and the Kwon-Chang [20] model based on the wall-attached bubble coalescence were originally developed for LWR operating conditions. The authors [4,19] suggested a procedure to predict the CHF for the HHF subcooled flow boiling and it was proven to be applicable to a wide range of operating conditions for both LWRs and fusion reactors. The Celata et al. model [2] based on the liquid sublayer dryout mechanism was originally developed for application to the HHF CHF.

Table 2. Parameter ranges of the mechanistic CHF models

	Celata et al. [2]	Weisman - Pei [3]	Kwon - Chang [20]
Pressure (MPa)	0.1 - 8.4	2 - 20.5	2 - 20
Mass flux (kg/m^2s)	900 - 90000	972 - 3611	450 - 7500
Diameter (mm)	0.3 - 25.4	1.15 - 37.5	1 - 37.5
Length (m)	0.0025 - 0.61	0.035 - 3.6	0.035 - 6
Subcooling	$\Delta T_{sub,in} \leq 225$ K	$\alpha < 0.6$	$\Delta h_{sub,in} \leq 1660$ kJ/kg
Used constants	No	3	1

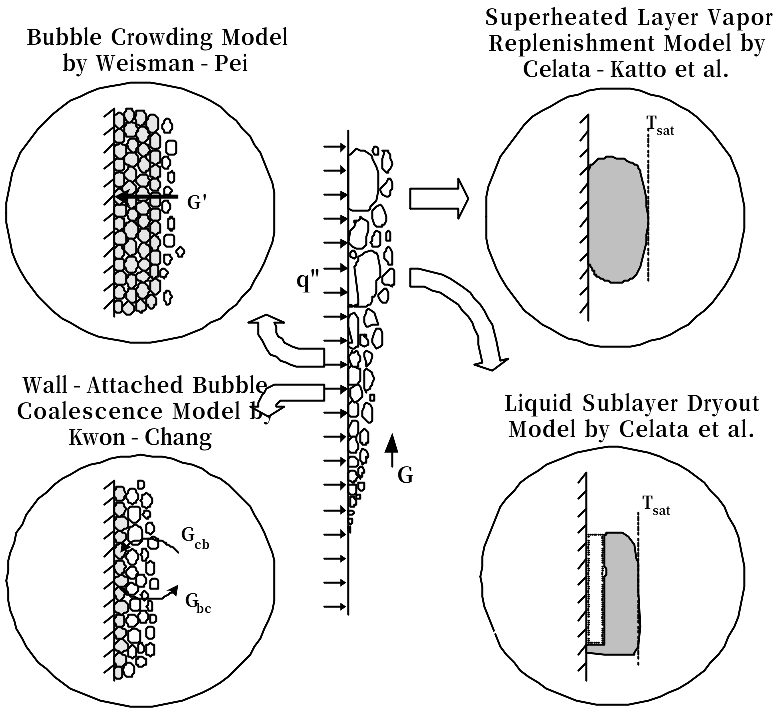

Fig.1 Concept of Mechanistic CHF Models

Table 2 shows the recommended ranges of variables for the chosen CHF models.

All the aforementioned models, except the Celata et al. model, contain some empirically determined constants to fit them against the experimental CHF data. The Kwon-Chang model contains one empirical correlation for the critical wall-void fraction. In the Weisman and Pei model, they adjusted an empirical constant of the density ratio of vapor and liquid in order to minimize the statistical error of the CHF predictions. The density difference becomes significantly large at low pressure and hence the empirical constant is not valid for low pressure. The Weisman and Pei model predicts the CHF well for only the high pressure region

3.2 Artificial Neural Network Method

The ANN has been utilized in many fields of engineering, e.g., pattern recognition, parameter estimation, control and so on. The ANN removes the burden of finding an appropriate model structure to fit the experimental data. Yapo et al. [5] and Moon and Chang [6] showed that an ANN might provide a valuable alternative to the current techniques for estimating the CHF. The back propagation network (BPN) is the most well known and widely used among the current neural network systems available. The

BPN learning algorithm is similar to human learning. A supervisor trains a network with pairs of problems and solutions. The BPN can then generalize the problem, extract their characteristics, and predict the solutions for untrained problems.

The general structure of the BPN network adopted in this application is shown in Fig. 2. Through a sensitivity study, a three-layered BPN was found to be more effective in predicting the CHF, which consists of one input layer, two hidden layers, and one output layer. Each layer is composed of nodes. External data enters the network through the input nodes and, after typically nonlinear transformations, the output data are generated by the output nodes. A detailed presentation of neural networks, as well as their application to predict the CHF, is presented in the reference papers.

The first step of the application of the BPN is to design a neural network that progresses all the available information. Selection of suitable input patterns is important for the BPN performance and they are constituted by the information on the channel geometry and the fluid conditions. Following the practice by Moon and Chang [6], five dimensionless parameters were chosen to correlate the CHF for the forced convection boiling in the uniformly heated vertical tubes as follows:

$$\frac{q_c''}{Gh_{fg}} = f\left(\frac{\rho_g}{\rho_f}, \frac{\sigma\rho_f}{G^2L}, \frac{L}{D}, \frac{\Delta h_{in}}{h_{fg}}\right) \qquad (1)$$

where q_c'' = CHF, G = mass flux, h = enthalpy, L = tube length, D = tube inside diameter, ρ = density, and σ = surface tension.

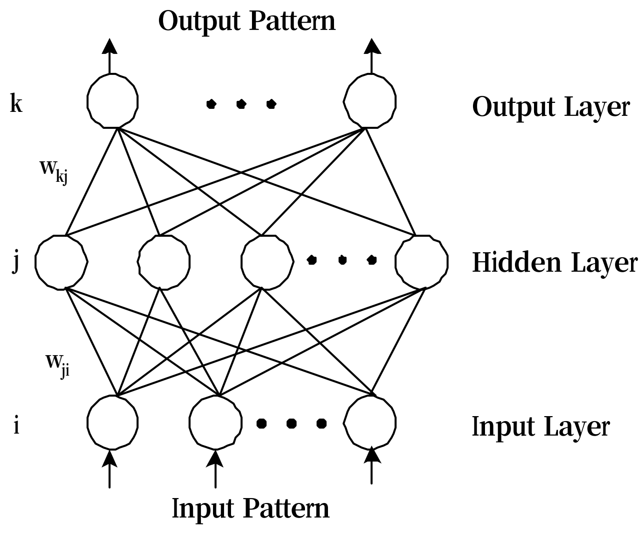

Fig. 2 The back-propagation neural network

The BPN is sensitive to the number of nodes in the hidden layer. After a sensitivity analysis, the node numbers of the first and second hidden layers are set to 30 and 40, respectively, in which 3000 iterations were done for network training. Since the task in the present application is to determine the CHF values with given conditions, the output layer is chosen to be made by a unique node.

In order to perform a reliable test of the BPN, the CHF database was subdivided into two subsets. About 90% of the CHF database was randomly selected and used to train the BPN. An error assessment of the trained BPN was then performed with the remaining data that were not used in the BPN training. Figure 3 shows the overall training and prediction procedures.

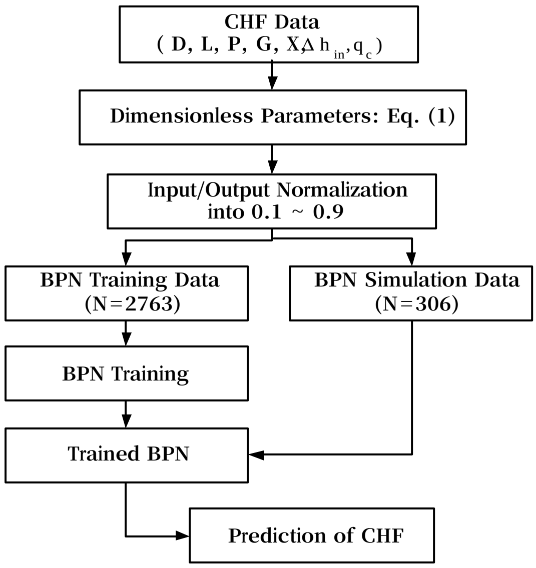

Fig. 3 BPN procedure for CHF prediction

4. Comparison with Experimental Data

Prediction by each CHF model was quantitatively evaluated by the CHFR, defined as the ratio of the predicted CHF to the measured CHF, with three statistical parameters of m (average value), s (sample standard deviation), and RMS (root-mean-square error) of the CHFR. The comparison was conducted for two data regions as discussed in the previous section: the HMSD region for $G \geq 10$ Mg/m^{2}s and $D < 3$ mm and the normal region for $G < 10$ Mg/m^{2}s or $D \geq 3$ mm.

It should be pointed out that the parameter ranges of the present database are outside the recommended ones for each CHF model shown in Table 2. The prediction performance by the mechanistic model is only good in the database range from which the model was validated. The purpose of analysis is to evaluate the generality of the CHF prediction method in the subcooled flow boiling. Table 3 shows the comparison results of the prediction performance against the present database, where the term original means the recommended range of the CHF model.

The Celata et al. model predicted about 89% of the 3069 data points within a ±30% error band. The model has a tendency to underpredict the CHF data for the present database as shown in Table 3. The Celata et al. model was developed using the ENEA database [18]. A total of 2167 data points out of 3069 fell into the recommended range of the model, and about 90% of which was predicted within a ±30% error band. The Weisman-Pei model generally over-predicted the CHF and the prediction performances by this model were not good in the low-pressure range as expected. If we restrict the experimental data to the recommended range, the Weisman-Pei model predicted a total of 999 data points with $\mu = 1.11$.

The Kwon-Chang model shows a relatively large discrepancy for the HMSD region, and 89% of the total 843 data points were predicted within a ±30% error band, while for the normal region, the model predicted fairly well, as shown in Fig. 4. About 90% of the 3069 experimental data were predicted within a ±30% error band. The assumptions and constitutive models that were employed in the construction of the

Table 3. Prediction performances by the mechanistic models and ANN method

	Type	No*	*m*	RMS	*s*
Celata et al.	HMSD	843	0.92	20.8	19.1
[2]	normal	2226	0.92	18.7	16.7
	total	3069	0.92	19.3	17.4
	original	2167	0.96	18.0	17.5
Weisman-	HMSD	843	1.16	26.3	20.6
Pei. [3]	normal	2222	1.21	28.9	19.7
	total	3065	1.20	28.2	20.1
	original	999	1.11	17.4	13.5
Kwon-	HMSD	843	0.99	22.0	22.0
Chang [4]	normal	2226	1.01	17.0	16.9
	total	3069	1.01	18.5	18.5
	original	886	1.02	10.4	10.0
ANN	HMSD	843	1.02	18.3	18.2
	normal	2226	1.025	10.9	10.6
	total	3069	1.02	13.3	13.1
Look-up Table [21]	normal	1575	0.99	17.4	17.3

* Number of CHF data successfully converged

mechanistic CHF model might not hold for a small tube diameter at a high mass flow rate (HMSD).

The BPN was trained by the 2063 data that were randomly selected. An error assessment of the trained BPN was then performed with the remaining 306 data that were not used in the BPN training. The comparison results for these untrained data points are shown in Fig. 5. The RMS errors of the prediction are 12.3%, of which a small error indicates that the training is successful and that the network is able to predict the CHF. The prediction results against the entire data are presented in Fig. 6.

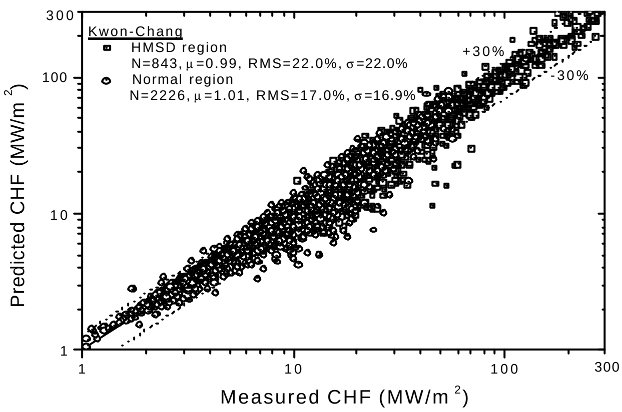

Fig. 4 Predicted vs measured CHF by the Kwon-Chang Model

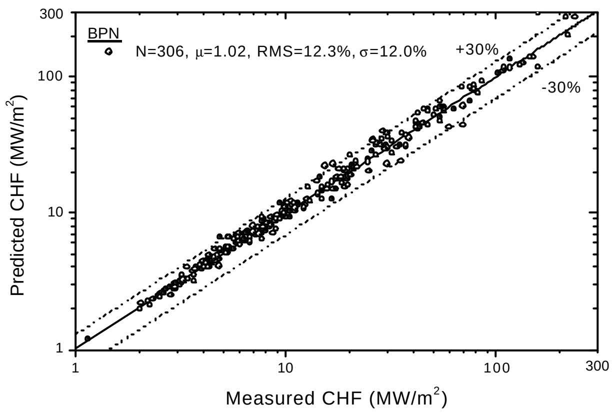

Fig. 5 Error assessment of the trained BPN

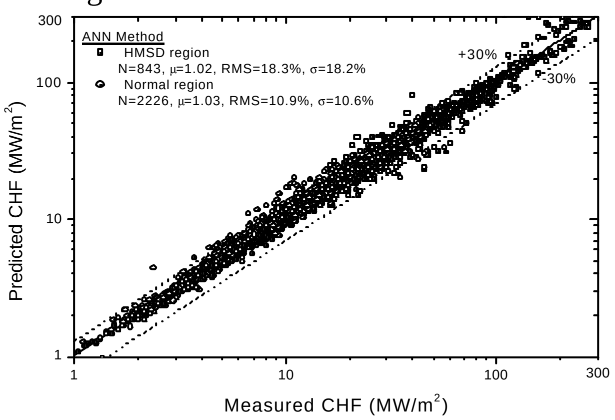

Fig. 6 Predicted vs measured CHF by the ANN

The predictions using the CHF look-up table of Groeneveld et al. [21] were performed based on the so-called heat balance method. The look-up table has its own applicable ranges, and only 1575 points out of 3069 were used for comparison. Since the upper limit of the mass flow rate is 8 Mg/m^{2}s, this method was not applicable to the HMSD region. For tube diameters other than 8 mm, the diameter correction equation suggested by the table authors was used. The average value of the CHFR is 0.99 with a standard deviation of 17.3 %. Figure 7 shows the comparison results of the 1575 data points by the CHF look-up table for the normal region.

The error distributions of the ANN and other CHF prediction methods are given in Figs. 8 and 9 for the HMSD and normal regions, respectively. Figure 10 shows the comparison of the percentage of data points calculated with the specific error range for the entire CHF data, where N means the number of data points successfully converged in the CHF calculation. Among the five CHF prediction methods considered here, the ANN gives the most accurate predictions for both ranges. For the HMSD region, the Kwon-Chang model is compatible with the Celata et al. model. For the normal region of the HHF subcooled flow boiling, the Kwon-Chang model gives the best prediction performance among the mechanistic models. It is interesting to see that the ANN method works well in comparison with the experimental data and the prediction performance is better than any other CHF prediction method considered here.

Based on the investigation of the dependence of the prediction accuracy on major parameters, the ANN method did not exhibit significant systematic deviations that could be attributed to certain system parameters, such as thermal-hydraulic conditions and geometric parameters. Experimentally, it has been clearly known that the subcooled flow boiling under conditions of high mass velocity and small tube diameter can accommodate very high heat fluxes. As shown in Figs. 11-12 for the normal region, the comparison of predictions by the

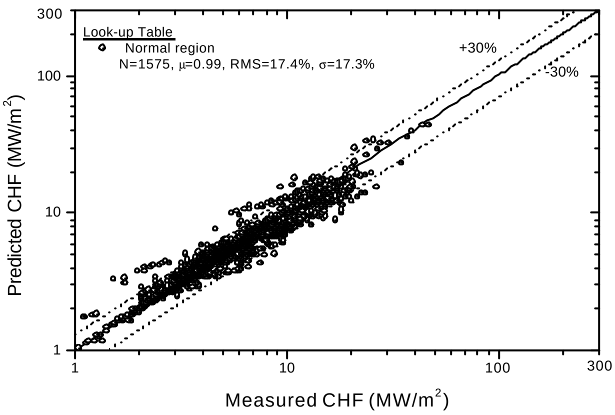

Fig. 7 Predicted vs measured CHF by the Look-up table

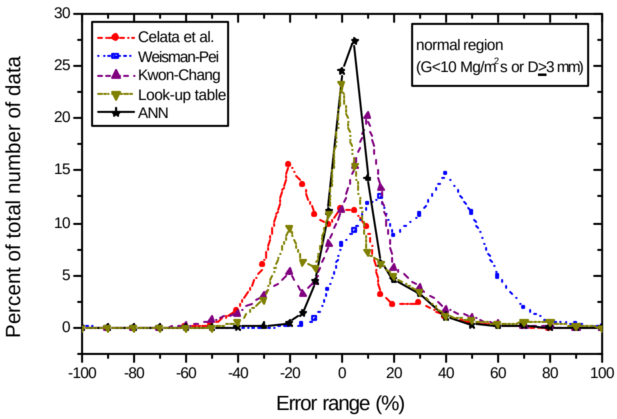

Fig. 8 Comparison of error distribution (normal region)

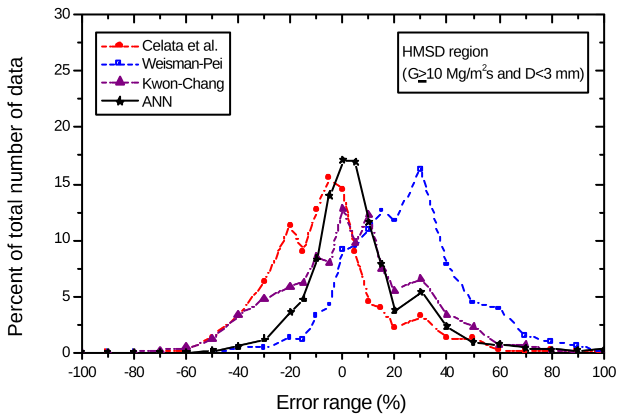

Fig. 9 Comparison of error distribution (HMSD region)

ANN method with the experimental data provided reliable accuracy. However, for the HMSD region, some scattering data points exist for very small or/and very high mass flow rate conditions.

5. Conclusion

A CHF prediction method using an ANN was evaluated for application to the HHF subcooled flow boiling. The ANN method utilized was based on the BPN technique. The developed ANN predictions were compared with the experimental database consisting of a total of 3069 CHF data points. The parameter ranges of experimental data were: $0.33 \leq D \leq 37.5$ mm, $0.002 \leq L \leq 4$ m, $0.37 \leq G \leq 134$ Mg/m^{2}s, $0.1 \leq P \leq 20$ MPa, $50 \leq \Delta h_{sub,in} \leq 1660$ kJ/kg, and $1.1 \leq q_{CHF} \leq 276$ MW/m^2.

When compared with the present high CHF database, the ANN method gave very accurate results with $\mu = 1.02$, $\sigma = 13.1\%$, and RMS=13.3%. Moreover, 91.5% of the total data points were predicted within ± 20%, which shows the best prediction performance among the existing CHF prediction methods considered. The ANN method is likely to be suitable for the HHF Subcooled flow boiling CHF.

Acknowledgment

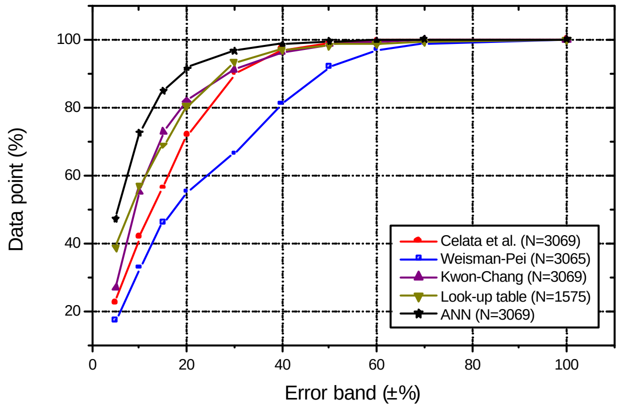

Fig.10 Comparison of prediction performance of various CHF

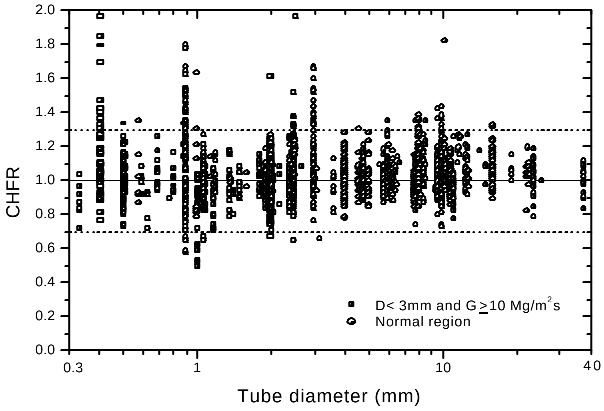

Fig. 11 CHFR vs tube diameter predicted by the ANN

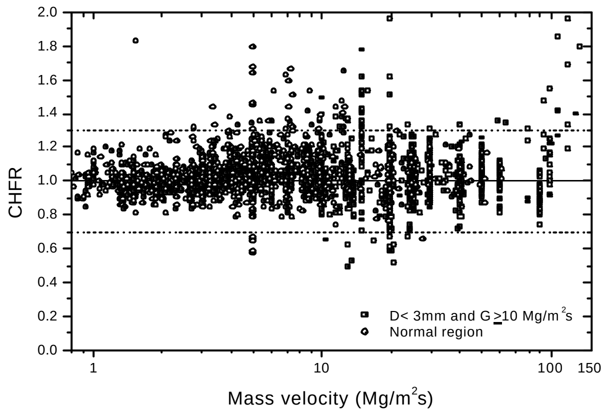

Fig. 12 CHFR vs mass flux predicted by the ANN

This work was performed under the long-term nuclear research and development program sponsored by the Korea Ministry of Science and Technology.

References

1. Kwon, Y.M. and Chang, S.H., A Procedure to Predict Subcooled-Water-Flow-Boiling CHF in Uniformly Heated Tubes for High-Heat-Flux Applications, Nucl. Tech., Vol.130 (to be issued in June, 2000).
2. Celata, G.P et al., Rationalization of Existing Mechanistic Models for the Prediction of Water Subcooled Flow Boiling Critical Heat Flux, Int. J. Heat Mass Transfer, Vol.37 (1994), pp.347-360.
3. Weisman, J. and Pei, B.S., Prediction of Critical Heat Flux in Flow Boiling at Low Qualities, Int. J. Heat Mass Transfer, Vol.26 (1983), pp.1463-1477.
4. Kwon, Y.M. and Chang, S.H., A Mechanistic Critical Heat Flux Model for High-Subcooling, High-Mass-Flux, and Small-Tube-Diameter Conditions, J. Korean Nucl. Soc., Vol.32 (2000), pp.17-33.
5. Yapo, T. et al., Prediction of Critical Heat Fluxes Using a Hybrid Kohonen-Backpropagation Neural Networks, Topics in Intelligent Engineering Systems Through ANNs, Vol.2, ed. Dali, C. H. et al. (1992).
6. Moon, S.K., Baek, W.P., and Chang, S.H., Parametric Trends Analysis of the Critical Heat Flux Based on Artificial Neural Networks, Nucl. Eng. Des., Vol.163 (1996), pp.29-49.
7. Bergles, A. E. et al., Critical Heat Flux and Flow Pattern Observations for Low Pressure Water Flowing in Tubes, J. Heat Transfer, Vol.69 (1967).
8. Nariai, H. and Inasaka, F., Critical Heat Flux and Flow Characteristics of Subcooled Flow Boiling with Water in Narrow Tubes, ed. Jones, O.C. and. Michiyoshi, I., Dynamics of Two-Phase Flows, CRC Press (1992), pp.689-708.
9. Mudawar, I. and Bowers, M.B., Ultra-High Critical Heat Flux (CHF) for Subcooled Water Flow Boiling - I: CHF Data and Parametric Effects for Small Diameter Tubes, Int. J. Heat Mass Transfer, Vol.42, (1999), pp.1405-1428.
10. Thompson, B. and Macbeth, R.V., Boiling Water Heat Transfer in Uniformly Heated Round Tubes: A Compilation of World Data with Accurate Correlations, AEEW-R-356 (1964).
11. Becker, K.M. et al., Round Tube Burnout Data for Flow of Boiling Water at Pressure Between 30 and 200 Bar, Report KTH-NEL-14 (1971).

12. Zenkevich, A., Analysis and Generalization of Experimental Data on Heat Transfer Crisis Associated with Forced Convection of Cooling Water in Tubes, AECL-Tr-Misc-304 (1974).
13. Chen, Y. et al., Critical Heat Flux with Subcooled Boiling of Water at Low Pressure, 8th Int. Topical Meeting on Nuclear Reactor Thermal-Hydraulics, Kyoto, Japan, Vol.2 (1997), pp.958-964.
14. Boyd, R.D., Subcooled Water Flow Boiling Experiments under Uniform High Heat Flux Conditions, Fusion Technology, Vol.13 (1988), pp.131-142.
15. Boyd, R.D., Subcooled Water Flow Boiling at 1.66 MPa under Uniform High Heat Flux Conditions, ASME Winter Annual Meeting, HTD Vol.119 (1989), pp.91-15.
16. Boyd, R.D., Subcooled Water Flow Boiling Transition and the L/D Effect on CHF for a Horizontal Uniformly Heated Tube, Fusion Tech., Vol.18 (1990), pp.317-324.
17. Nariai, H., Inasaka, F., and Kinoshita, H., Critical Heat Flux of Subcooled Flow Boiling with and without Internal Twisted Tape under Circumferentially Non-Uniform Heating Condition, Proc. German-Japanese Sympo. on Multiphase Flow, (1994), pp.191-205.
18. Celata, G.P., Cumo, M., and Mariani, A., Assessment of Correlations and Models for the Prediction of CHF in Water Subcooled Flow Boiling, Int. J. Heat Mass Transfer, Vol.37 (1994), pp.237-255.
19. Kwon, Y.M. and Chang, S.H., Evaluation of Prediction Models for Subcooled Water flow Boiling CHF for High-Heat-Flux Applications, ICONE-8, Baltimore, USA (2000)
20. Kwon, Y.M. and Chang, S.H., A Mechanistic Critical Heat Flux Model for Wide Range of Subcooled and Low Quality Flow Boiling, Nucl. Eng. Des., Vol.188 (1999), pp.27-47.
21. Groeneveld, D.C. et al., The 1995 Look-up Table for Critical Heat Flux in Tubes, Nucl. Eng. Des., Vol. 163 (1996), pp.1-23.